may be considered to occur when the primary energy is so low that if the primary shares its energy with a second electron, neither electron will have sufficient energy to escape from the target. It was previously pointed out in the discussion of Fig. 3 and Fig. 4 that this occurs for Mo when V_p is less than 5 volts and for W when V_p is less than 7 volts. Only elastic reflection of primary electrons occurs for V_p values lower than these. Between these two extreme cases lies a transitional region which appears from the experiment to be about 10 or 12 volts wide in terms of V_p. The transition is evident in Figs. 5, 6, and 7. In this region it is possible for the primary to undergo a small number of scatterings —probably one or two—and still retain sufficient energy to be able to escape. For V_p greater than 20 volts, statistical theories can be applied but for lower V_p values, single processes must be considered and appropriate theoretical treatment is not available at the present time.

ACKNOWLEDGMENTS

It is a pleasure to acknowledge my gratitude to F. S. Best, A. A. Machalett, V. J. DeLucca, and H. C. Meier, who contributed to the construction of the apparatus, and to R. A. Maher, who assisted in all phases of the experimental work. I would also thank H. D. Hagstrum and P. A. Wolff who generously provided some very helpful discussion.

PHYSICAL REVIEW VOLUME 104, NUMBER 1 OCTOBER 1, 1956

Multiple Ferromagnetic Resonance in Ferrite Spheres

ROBERT L. WHITE AND IRVIN H. SOLT, JR.
Hughes Research Laboratories, Culver City, California

(Received May 8, 1956)

Ferromagnetic resonance experiments have been performed on single crystal spheres of manganese and manganese-zinc ferrites placed in field configurations having large gradients in the rf magnetic field at the sample site. Five major and several minor resonant absorptions are observed extending over a region of 700 oersteds at room temperature. The line spacings are essentially independent of sphere size. The absorptions are shown to be attributable to modes of precession of the bulk magnetization of the sample which are more complicated than the spatially uniform precession contemplated by the usual ferromagnetic resonance theory. The lowest order modes are identified and their dynamical properties shown to be consistent with the prediction of an idealized magnetically-coupled-oscillator model.

INTRODUCTION

THE phenomenon of ferromagnetic resonance has been much used as a tool for the investigation of the magnetic properties of ferrite materials. The variation with crystallographic orientation of the field required for resonance yields the crystalline magnetic anisotropy constants. The field for resonance corrected for anisotropy effects gives the magnetic g factor. Perhaps most important, the half-width of the resonance in ω or in H may be interpreted according to the theory of Bloembergen[1] or of Landau and Lifshitz[2] to give the characteristic relaxation time of the magnetic system.

Two problems pertaining to this last property have for several years puzzled investigators using conventional ferromagnetic resonance techniques: First, why is it an experimental fact that the resonant absorption is often far from symmetric in shape and may even exhibit clearly defined secondary maxima, especially for larger sample sizes? Second, why are the relaxation times inferred from the line widths so short?

The answer to the first question is contained in the work reported here. Higher modes of ferromagnetic resonance, in which the precessional phase varies from point to point within the sample, are shown to exist and to have fields for resonance in general different from the Kittel value.[3] The "distorted" line shapes and "spurious" secondary maxima may be explained as caused by the accidental excitation of the higher modes of resonance.

Though the answer to the second question is far from contained in the work below, some strong clues are present. Coupling of the ferromagnetic resonance mode of uniform precessional phase to nearly degenerate modes of much higher order may be of great significance in the relaxation process.

APPARATUS

The experimental apparatus used for the resonant absorption measurements is similar in many respects to the recording system described by Tinkham, Solt, Davis, and Strandberg.[4] The system consists of two

[1] N. Bloembergen, Phys. Rev. **78**, 572 (1950).
[2] L. Landau and E. Lifshitz, Physik. Z. Sowjetunion **8**, 153 (1935).
[3] C. Kittel, Phys. Rev. **73**, 155 (1948).
[4] Strandberg, Tinkham, Solt, and Davis, Rev. Sci. Instr. **27**, 596 (1956).

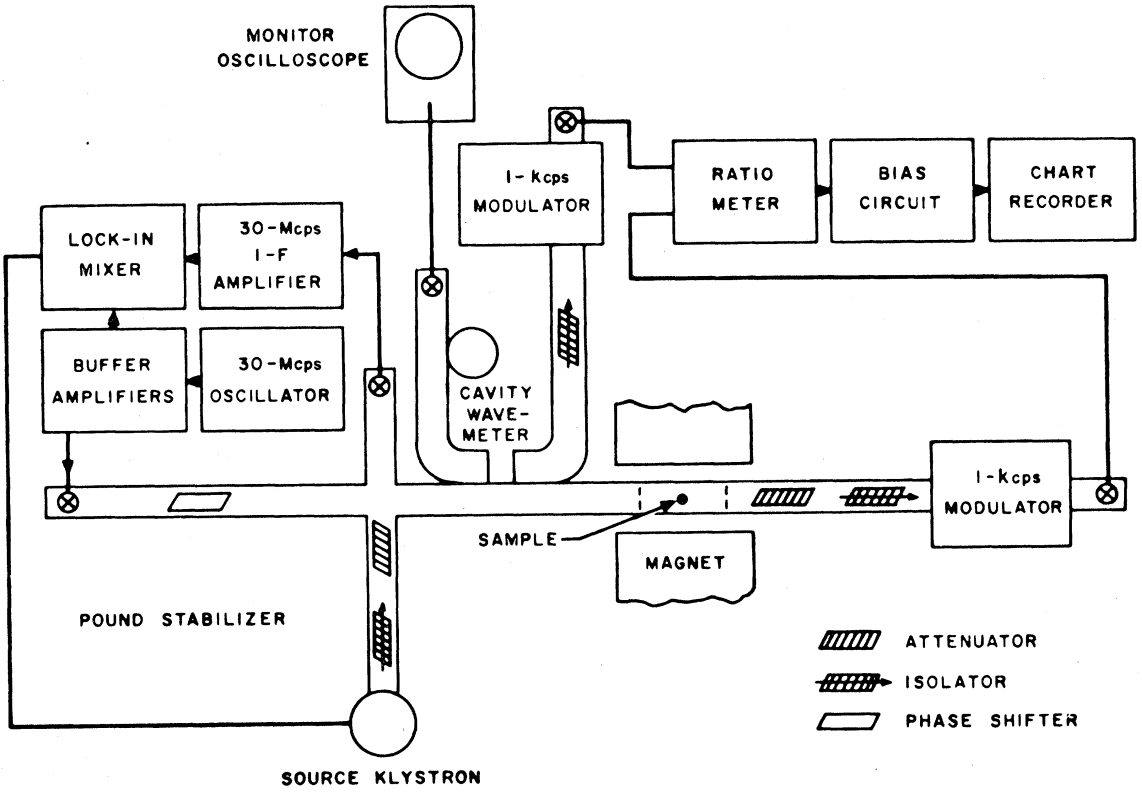

FIG. 1. Block diagram of microwave and detection apparatus.

basic units, the magnetic field sweep system and the microwave and detection circuits.

In the magnetic field stabilization system, a rotating flip coil continuously monitors the magnetic field. The voltage induced in this flip coil is compared with a fraction of the voltage from a reference generator which is driven by the same motor that drives the flip coil. The comparison voltage is amplified, synchronously detected, amplified further, and applied directly to the grids of the series tubes in the power supply of the 6-inch Varian magnet. A parallel channel of current feedback is included to improve stability. To sweep the magnetic field linearly in time, a helipot supplying the comparison voltage from the reference generator is driven by a geared-down synchronous motor.

Absorption of microwave energy by the sample may be measured by observing the change in transmission or reflection coefficient of a resonant cavity containing the sample. For small incremental absorptions, such as are encountered in paramagnetic resonance, both cavity transmission and reflection coefficients vary linearly with absorption. However, for the large absorption encountered in ferromagnetic resonance this approximation is not valid and it was necessary to develop distinctly different and unique instrumentation. For the source tuned to cavity resonance, one can readily derive the exact relation

$$P_a=\frac{1}{Q_L}\left[\left(\frac{T_0}{T}\right)^{\frac{1}{2}}-1\right], \tag{1}$$

where P_a is the power absorbed by the sample, Q_L is the loaded Q of the empty cavity, T_0 is the power transmission coefficient of the empty cavity, and T is the transmission coefficient of the cavity containing the ferrite. Hence for a recording system to plot directly the sample absorption, it is necessary to have a transmission cavity, a square law microwave power detector, an instrument to extract the square root of the ratio of two voltages, and appropriate biasing circuits to subtract the constant factor in Eq. (1).

Figure 1 shows a block diagram of the apparatus. A TE_{10n} rectangular transmission cavity was used. For these experiments, n varied from 1 to 6. The source klystron was stabilized directly to the absorption cavity. For the X-band work, Narda type 610B bolometers were found to be reliable and convenient square law detectors; crystals may also be used, but great pains must be taken to make them square law over the power range being used by varying the load impedance seen by the crystal. The requirement of extracting the square root of the ratio of two voltages was met by the Hewlett-Packard type 416A ratio

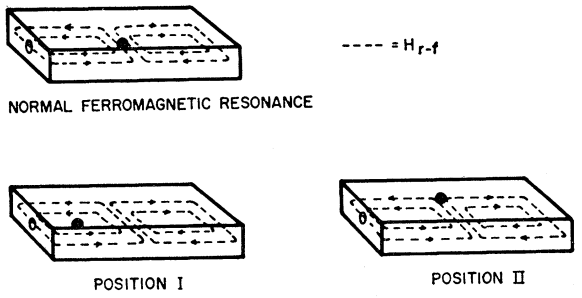

FIG. 2. Positioning of sample in TE_{102} cavity for ferromagnetic resonance experiments.

meter, an instrument designed primarily for microwave reflectometer measurements. The quantity T_0 of Eq. (1) is simulated by a sampling of the incident power whose level can be set to equal the transmitted power for an empty cavity. Obtaining T_0 in this fashion gives the added advantage of normalizing the ratio against changes in the microwave power level that occur as a result of the change in output of the klystron with frequency. The output of the ratio meter is connected through a biasing circuit directly to the chart recorder which plots the absorption.

In order to obtain the symmetries of the microwave fields required to drive the various resonant precessional modes, it was necessary to vary the sample position within the cavity. In most experiments the needed variation was instrumented by glueing the ferrite sphere to a Saran thread run through small holes in the cavity walls. Continuous positional variation in several directions could thus be accomplished. For the measurements at elevated temperatures a cavity with heating coils wound directly upon it was used. In these measurements only certain discrete sample positions were used, each accomplished with the proper length quartz rod stand-off mounted on a plug inserted in the cavity wall. Figure 2 shows the sample positions most commonly used.

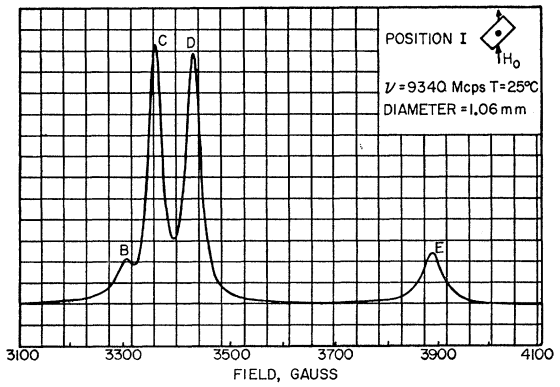

FIG. 3. Multiple ferromagnetic resonance in manganese-zinc ferrite-position I.

EXPERIMENTAL RESULTS

The general patterns of ferromagnetic resonance absorptions observed consist of five major lines, denoted components A through E, and a number of minor lines. Figure 3 shows the absorptions observed at room temperature for a manganese-zinc ferrite sphere in position I as defined in Fig. 2. Figure 4 shows the pattern for the sphere moved to position II as defined in Fig. 2. It may be observed that in position II components D and E have disappeared while component A has appeared and component B is greatly enhanced. The patterns for manganese ferrite under similar circumstances are qualitatively identical. By using the proper sample position within the cavity and selecting the orientation of the external magnetic field, H_z, it is possible to excite the absorptions separately or in subgroups. Component E, for instance, appears only when the components of rf magnetic field perpendicular to H_z have gradients in the direction of H_z.

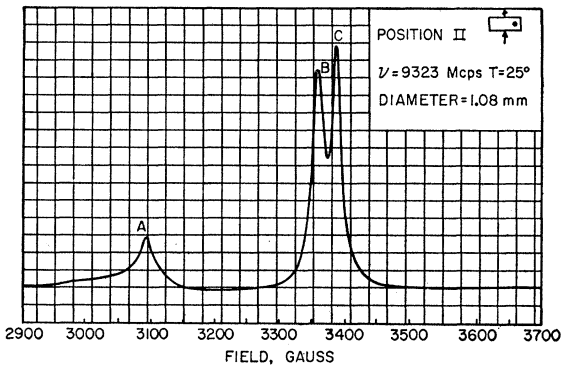

FIG. 4. Multiple ferromagnetic resonance in manganese-zinc ferrite-position II.

At a given frequency, the positions of the resonances are to a first approximation independent of sphere size over the range of sizes from 0.65-mm diameter to 1.33-mm diameter. Except for component C, the magnitudes of the absorptions decrease with sphere size considerably more rapidly than the sample volume. At the larger sphere sizes, a number of additional resonances of yet stronger dependence on sample radius become visible. They are interspersed among components A through E, which are of primary concern here. Over the range of frequencies convenient with X-band apparatus, from 8.1 to 10 kMc/sec, the pattern shows only a very weak dependency on frequency, the lines changing at most a few gauss in relative position. At K_a band, about 34 kMc/sec, components B and D change considerably but components A, C, and E preserve approximately their spacings.

The line intervals at X-band do exhibit, however, a strong, fairly complicated dependence on temperature. The data are shown in Figs. 5 and 6 for Mn-Zn and

Mn ferrites, respectively. Attention is particularly invited to the behavior of components B and D.

ORIGIN AND CLASSIFICATION OF RESONANCE

The resonances observed in these experiments can be excited separately or in subgroups by choosing the appropriate orientation of H_z and proper symmetry of the exciting microwave field. This behavior strongly suggests that the sphere oscillates in modes of definite symmetry. Further, the observed dependence of line spacings on temperature suggests that the mechanism of mode splitting is intimately related to the magnitude of M the saturation magnetization.

Consider the idealized conventional ferromagnetic resonance experiment. A ferrite sphere is placed in a strong steady magnetic field H_z, then subjected to a uniform rf magnetic field H_1 in a plane perpendicular to H_z. The magnetization-bearing spins throughout the sample will precess about H_z with uniform phase. If, however, H_1 is not uniform across the sample, but is, say, in opposite directions at opposite ends of a diameter the spins will try to precess in different phase and amplitude at different points in the sample. Such spatially nonuniform precessional modes are responsible for the multiple resonant absorptions under discussion. For small precession amplitude, spins at different positions will be coupled to one another primarily through the divergence in M produced by the nonuniform precession.

Component E characteristically appears when the component of H_1 perpendicular to H_z has a gradient in the direction of H_z. With H_z vertical, then, top and bottom halves of the sphere are driven in opposite phase. Top and bottom are driven at the same frequency and the "bent" magnetization precesses as a unit but has a different field for resonant precession than the unbent magnetization due to the torque one hemisphere exerts on the other.

Components A through D characteristically appear when the components of H_1 orthogonal to H_z and to one another have gradients in the plane perpendicular to H_z. One is led by the symmetries of the driving fields to suspect that the absorption results from the magnetization of the sphere precessing in quarter segments. To facilitate calculation of the properties of such a system, the situation has been idealized into four magnetic dipoles, representing the lumped bulk magnetization of the quadrants, in square array, with the steady field H_z perpendicular to the plane of the square. The dynamic properties of such a system are calculated in the appendix. The four characteristic frequencies of the system are

$$\omega_A^2=\gamma^2[H_z+2(A'-B')]^2, \quad (2)$$

$$\omega_B^2=\gamma^2[H_z+2(A'-B'')][H_z-2(B'-A'')], \quad (3)$$

$$\omega_C^2=\gamma^2 H_z^2, \quad (4)$$

$$\omega_D^2=\gamma^2[H_z+2(A'+A'')][H_z-2(B'+B'')], \quad (5)$$

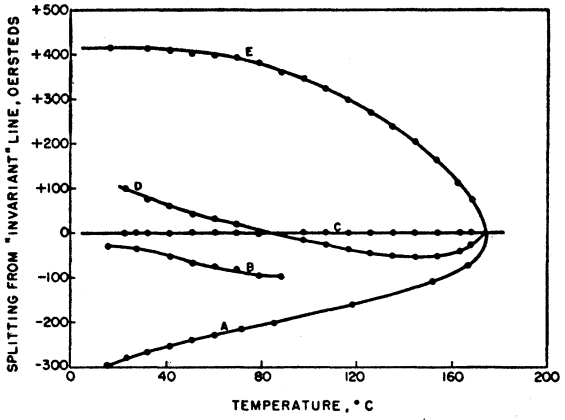

FIG. 5. Field splitting of ferromagnetic resonance lines as a function of temperature for manganese-zinc ferrite.

where A', B', A'', B'' are torque constants defined in the appendix.

For comparison with the experimental results, one can express these roots in terms of the field H_z required for resonance at a fixed frequency. In Fig. 7, the field for resonance for the various components is plotted as a function of coupling strength (probably nearly proportional to M). The assumptions have been made that $A>B$, $A'>A''$, $B'>B''$, and the coupling constants all increase at the same rate. Comparison with Figs. 5 and 6 reveal good, almost quantitative, agreement with the experimental data, when the known dependence of M on temperature is used and the coupling strength is assumed proportional to M. Since the line intervals are somewhat dependent on crystal orientation and since the model was oversimplified, more detailed evaluation of the coupling constants and other parameters for best fit does not seem warranted.

The normal coordinates of the characteristic modes of the four coupled oscillators may also be obtained from Eq. (A-10) of the appendix. In each instance the symmetry of the normal coordinates corresponds to

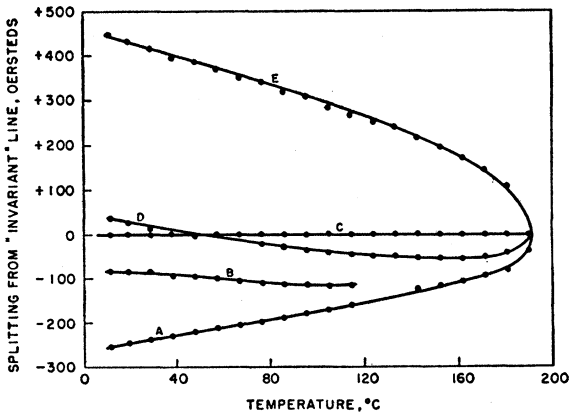

FIG. 6. Field splitting of ferromagnetic resonance lines as a function of temperature for manganese ferrite.

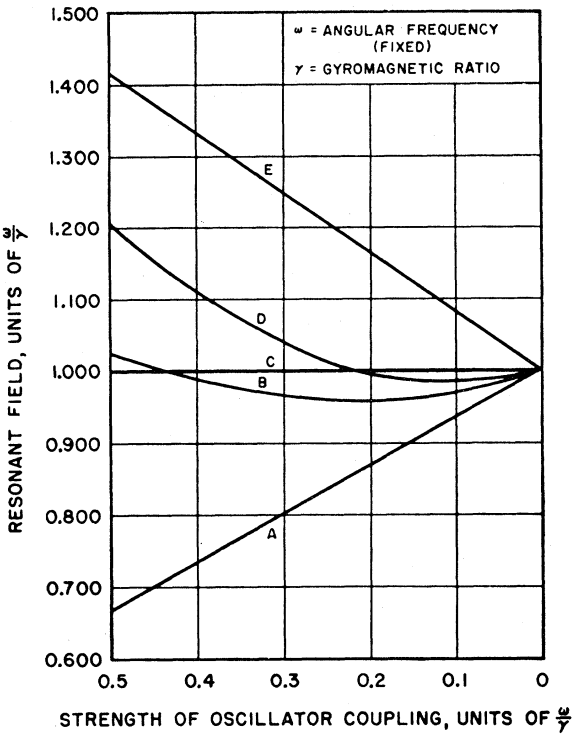

FIG. 7. Plot of field for resonance for various coupled-dipole modes as a function of coupling strength.

the symmetry of the microwave magnetic field required to selectively excite the mode. This correspondence confirms the mode assignment indicated above and provides additional confirmation of the validity of the model.

DISCUSSION

The manganese and manganese-zinc ferrites used in the experiments are characterized by a large saturation magnetization and long ferromagnetic relaxation time (5×10^{-9} sec). Consequently, the dominant lower order precessional modes appear mostly as fully resolved resonances. For ferrites of smaller M and shorter relaxation time (hence, greater line width), the various resonant modes will be unresolved and a composite absorption observed. The presence of the unresolved sub-structure explains the size-dependent line shapes reported by many observers.[5–7] Dimensional resonances, in which the ferrite sphere behaves as a dielectric cavity,[5] appear to play no part in the phenomenon.

The line widths in Figs. 3 and 4 merit comment in themselves. In the manganese-zinc ferrite, component C, attributable to the spatially uniform mode, exhibits a room-temperature line width varying from 18 to 20 oersteds with crystallographic orientation. This width is somewhat less than half that of the narrowest lines observed by Tannenwald[8] or by Dillon, Geschwind, and Jaccarino,[7] in compositionally similar material from the same source.[9] It is also of interest to note that the first order anisotropy constant K_1/M for the sample of Figs. 3 and 4 is approximately 35 oersteds, this quantity also being somewhat less than half that observed by Tannenwald or Dillon *et al.* for their crystals.

The theory of line widths in ferromagnetic resonance is strongly affected by the existence of the higher order precessional modes. The most successful attacks on the problem of ferromagnetic relaxation have been phrased in the language of spin waves,[10] an approximation one would expect to be valid at temperatures below about one-tenth the Curie temperature. Clogston, Suhl, Walker, and Anderson[11] have recently shown that for most sample geometries, including the sphere, there exists a surface in k space of spin waves of high k which are degenerate with the spin wave of $k=0$ excited in a ferromagnetic resonant experiment. Further, it had previously been demonstrated that spin waves of high k interact strongly with the crystal lattice and have a half-life on the order of the relaxation times observed for ferromagnetic resonance, about 10^{-9} sec. The mechanisms which could scatter the spin waves of $k=0$ into those of higher k are numerous if no energy promotion is required. A two-stage relaxation process is therefore established in which both stages proceed at rates comparable to the experimentally observed relaxation times.

The precessional modes of higher order are the conceptual equivalent of the spin waves of higher k. The coupled oscillator model presented in this paper suffices only for certain lower order modes, but the properties of modes of arbitrarily high order may be derived from the gyromagnetic equation and proper boundary conditions.[12] These rest only on Maxwell's equations and present a picture clearly valid over the range of temperatures of interest. Only preliminary results of these calculations are available, but the indication is that there are numerous modes of higher order degenerate or nearly degenerate with the uniform

[5] Yager, Galt, Merritt, and Wood, Phys. Rev. **80**, 744 (1950).
[6] D. W. Healy, Jr., Cruft Laboratory, Harvard University, Technical Report No. 135, 1951 (unpublished).
[7] Dillon, Geschwind, and Jaccarino, Phys. Rev. **100**, 750 (1955).
[8] P. E. Tannenwald, Phys. Rev. **100**, 1713 (1955).
[9] Single crystal ferrites obtained from Linde Air Products Company through the courtesy of Dr. R. W. Kebler and Dr. G. W. Clarke.
[10] T. Holtstein and H. Primakoff, Phys. Rev. **58**, 1098 (1940); A. Akheiser, J. Phys. (U.S.S.R.) **10**, 217 (1946); F. Keffer, Phys. Rev. **88**, 686 (1952). C. Kittel and E. Abrahams, Revs. Modern Phys. **25**, 233 (1953).
[11] Clogston, Suhl, Walker, and Anderson, Phys. Rev. **101**, 903 (1956). We are indebted to the above authors for preprints of this article and of reference 12, and for discussions concerning the subject matter therein.
[12] L. R. Walker, Bull. Am. Phys. Soc. Ser. II, **1**, 125 (1956).

mode. The coupling of energy into these modes constitutes an important step in the relaxation process.

As a final point of discussion, it should be observed that the multiple resonances treated here are not the low-field secondary maxima observed by Kip and Arnold[13] or by Bickford[14] or Tannenwald.[8] These observers were dealing with multiple domain situations in magnetically unsaturated materials. The pertinent theory under these circumstances has been given by Smit[15] and Artman.[16]

ACKNOWLEDGMENTS

The authors wish to express their gratitude to Mr. James E. Mercereau for his assistance in both the theoretical and experimental aspects of the project, and to Dr. Bela A. Lengyel for helpful discussion and criticism.

APPENDIX

Consider the dynamic system composed of four magnetic dipoles, $\mathbf{M}_i$, in a square array situated in a strong external magnetic field $\mathbf{H}$ perpendicular to the plane of the square. The coupling between dipoles will not be taken to be the classical point dipole-point dipole interaction since these dipoles represent the lumped bulk magnetization of four spherical segments. We define instead a compressional torque constant A and a shear torque constant B as follows: Let two dipoles initially parallel be bent towards one another, each through a small angle θ [Fig. 8(a)]. The restoring torque perpendicular to their common plane acting on either is defined to be $2A\theta$. If the two dipoles

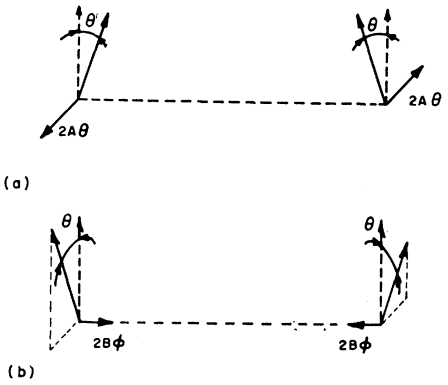

FIG. 8. Diagram illustrating definition of torque constants.

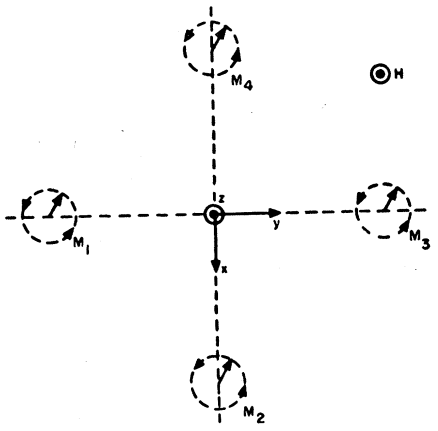

FIG. 9. Diagram illustrating coordinate system for coupled oscillator calculation.

are bent out of their common plane in a shear fashion through small angles ϕ [Fig. 8(b)] the torque on either is $2B\phi$, in their common plane. Both A and B will be positive quantities as drawn in Fig. 1. In the subsequent calculation singly primed torques will refer to nearest neighbor interactions; doubly primed, to interaction between diagonally situated dipoles.

The gyromagnetic equations of motion will be

$$\frac{1}{\gamma}\frac{\partial \mathbf{M}_i}{\partial t}=\mathbf{M}_i\times\mathbf{H}+\sum_{j\neq i}\mathbf{T}_{ij}. \tag{A-1}$$

The torque exerted by the jth dipole upon the ith is represented by $\mathbf{T}_{ij}$.

We establish a coordinate system and dipole designation as shown in Fig. 9. For small amplitudes of oscillation about the equilibrium position,

$$\mathbf{M}_i=m_{ix}\exp[i\omega t]\mathbf{i}+m_{iy}\exp[i\omega t]\mathbf{j}+M\mathbf{k}, \tag{A-2}$$

where

$$m_{ix},\quad m_{iy}\ll M,\quad \mathbf{H}=H_z\mathbf{k} \text{ throughout.}$$

We can now write explicit expressions for the T_{ij}; for example,

$$(T_{12})_x=\tfrac{1}{2}(A'+B')(m_{1x}-m_{2x})/M +\tfrac{1}{2}(A'-B')(m_{1y}-m_{2y})/M, \tag{A-3}$$

or

$$(T_{13})_y=B''(m_{1x}-m_{3x})/M.$$

Using the further shorthand notation,

$$\tfrac{1}{2}(A'+B')=C \quad\text{and}\quad \tfrac{1}{2}(A'-B')=D, \tag{A-4}$$

we can write the system of Eqs. (A-1)

$$\mathbf{P}\cdot\mathbf{u}=0, \tag{A-5}$$

where $\mathbf{P}$, the coefficient matrix, after introduction of

[13] A. F. Kip and R. D. Arnold, Phys. Rev. **75**, 1556 (1949).
[14] L. R. Bickford, Laboratory for Insulation Research, Massachusetts Institute of Technology, Technical Report No. 23, 1949 (unpublished).
[15] J. Smit, Philips Research Repts. **10**, 113 (1955).
[16] J. O. Artman, Lincoln Laboratory Report, March, 1956 (unpublished).

the abbreviation, $H_D=H_z+2D$, is

$$\begin{bmatrix} -i\omega/\gamma & H_D+A'' & -C & -D & O & -A'' & C & -D \\ -(H_D-B'') & -i\omega/\gamma & D & C & -B'' & O & D & -C \\ -C & -D & -i\omega/\gamma & H_D-B'' & C & -D & O & B'' \\ D & C & -(H_D+A'') & -i\omega/\gamma & D & -C & A'' & O \\ O & -A'' & C & -D & -i\omega/\gamma & H_D+A'' & -C & -D \\ -B'' & O & D & -C & -(H_D-B'') & -i\omega/\gamma & D & C \\ C & -D & O & B'' & -C & -D & -i\omega/\gamma & H_D-B'' \\ D & -C & A'' & O & D & C & -(H_D+A'') & -i\omega/\gamma \end{bmatrix}, \tag{A-6}$$

and

$$\mathbf{u}=\begin{bmatrix} m_{1x} \\ m_{1y} \\ \cdot \\ \cdot \\ \cdot \\ m_{4y} \end{bmatrix}. \tag{A-7}$$

The equations of motion can be put in a much more suggestive form by the unitary transformation

$$\mathbf{T}=\tfrac{1}{2}\begin{bmatrix} 1 & 0 & 1 & 0 & 1 & 0 & 1 & 0 \\ 0 & 1 & 0 & 1 & 0 & 1 & 0 & 1 \\ 1 & 0 & -1 & 0 & 0 & -1 & 0 & -1 \\ 0 & 1 & 0 & -1 & 1 & 0 & -1 & 0 \\ 1 & 0 & 1 & 0 & -1 & 0 & -1 & 0 \\ 0 & 1 & 0 & 1 & 0 & -1 & 0 & -1 \\ 1 & 0 & -1 & 0 & 0 & 1 & 0 & -1 \\ 0 & 1 & 0 & -1 & -1 & 0 & 1 & 0 \end{bmatrix}. \tag{A-8}$$

This transformation reduces the coefficient matrix to four two-by-two matrices on the principal diagonal. The equation

$$(\mathbf{T}^{-1}\mathbf{P}\mathbf{T})\mathbf{T}^{-1}\mathbf{u}=0 \tag{A-9}$$

can then be written in reduced form,

$$\begin{aligned} \begin{pmatrix} -i\omega/\gamma & H_z \\ -H_z & -i\omega/\gamma \end{pmatrix}\begin{pmatrix} m_{1x}+m_{2x}+m_{3x}+m_{4x} \\ m_{1y}+m_{2y}+m_{3y}+m_{4y} \end{pmatrix}&=0, \\ \begin{pmatrix} -i\omega/\gamma & H_z+4D \\ -(H_z+4D) & -i\omega/\gamma \end{pmatrix}\begin{pmatrix} m_{1x}-m_{2x}+m_{3x}-m_{4x} \\ m_{1y}-m_{2y}+m_{3y}-m_{4y} \end{pmatrix}&=0, \\ \begin{pmatrix} -i\omega/\gamma & H_z+2(D+C+A'') \\ -[H_z+2(D-C-B'')] & -i\omega/\gamma \end{pmatrix}\begin{pmatrix} m_{1x}+m_{2y}-m_{3x}-m_{4y} \\ m_{1y}-m_{2x}-m_{3y}+m_{4x} \end{pmatrix}&=0, \\ \begin{pmatrix} -i\omega/\gamma & H_z+2(D-C+A'') \\ -[H_z+2(D+C-B'')] & -i\omega/\gamma \end{pmatrix}\begin{pmatrix} m_{1x}-m_{2y}-m_{3x}+m_{4y} \\ m_{1y}+m_{2x}-m_{3y}-m_{4x} \end{pmatrix}&=0. \end{aligned} \tag{A-10}$$

One can now obtain almost by inspection the roots of the secular equation derived from the condition that the determinant of the coefficient matrix must vanish. These roots are

$$\begin{aligned} \omega_1^2&=\gamma^2H_z^2, \\ \omega_2^2&=\gamma^2[H_z+2(A'-B')]^2, \\ \omega_3^2&=\gamma^2[H_z+2(A'+A'')][H_z-2(B'+B'')], \\ \omega_3^2&=\gamma^2[H_z+2(A'-B'')][H_z-2(B'-A'')]. \end{aligned} \tag{A-11}$$

Furthermore, the transformed basis vectors, $\mathbf{T}^{-1}\mathbf{u}$, give the normal coordinates of the oscillations.